Effectiveness and optimization strategies of passive design adapting to climate change for high-rise apartments in hot and humid Philadelphia

Zhen Lei[1], Yue Fang[2]

[1]School of Design, University of Pennsylvania, Philadelphia, U.S. (Zhen_Lei@outlook.com)

[2]College of Engineering, Northeastern University, Boston, U.S.

Abstract.

For architectural design to actualize climate adaptation, it is essential to optimize building energy efficiency, emission reduction, and passive survivability. However, the effectiveness and thermal comfort demand of passive design strategies for building retrofit in hot and humid climates are limited in current literature research. Moreover, as an emerging design technology, building energy simulation and optimization (BESO) has not been widely applied in architectural practice due to its long calculation time and lack of a unified standard method. This paper aims to explore the effectiveness and optimization strategies of passive design for the residential building type in hot and humid climates, considering the dynamic effects of energy consumption, thermal comfort, and future climate scenarios. In this study, the developed future weather data file was used to plot the Givoni bioclimatic chart (GBC), and the data set was constructed based on the EnergyPlus model simulation. Meanwhile, the optimal solutions are realized based on the Morris sensitivity analysis (SA) method and the NSGA-II algorithm. Through the application workflow ranging from climate analysis to performance simulation and effectiveness validation, it provides passive design strategies for a typical high-rise apartment retrofit in Philadelphia. The results indicate that in the current subtropical humid environment, window ventilation strategies remain effective in reducing cooling loads and improving thermal comfort. In future high-humidity and high-temperature climates, solar protection and high-performance envelope structures will become important factors in achieving energy efficiency and ensuring the threshold for passive survivability. Through simulation optimization considering different climate scenarios, the combination of design parameters can reduce annual energy consumption by up to 40%, decrease both cooling and heating loads by over 50%, and improve thermal comfort by over 30%.

Keywords: passive design, energy efficiency, thermal comfort, sensitivity analysis, multi-objective optimization

1. Introduction

1.1 Background of this study

The trend of global warming and the frequency of extreme weather have begun to make architectural design focus on ecosystems, biodiversity, and human settlements at the regional level. In developed countries in Europe and North America, building energy consumption accounts for

about 40% of the total energy consumption (IEA-ISO, 2012). Energy efficiency and integrated technology have become hot topics at the forefront of contemporary international research trends. Climate adaptation has been introduced into topics such as architectural vulnerability and urban resilience.

Philadelphia lies between the subtropical humid climate zone and the temperate continental humid climate zone, with four distinct seasons and a relatively even distribution of precipitation, which has the typical climate characteristics of hot summer cold winter (HSCW) (Kottek et al., 2006). Currently, the passive design has been proven the effectiveness in energy efficiency and thermal comfort in high-rise residential buildings in hot and humid areas through external shading, natural ventilation, and thermal insulation materials.

1.2 Gaps and aims of this study

The existing passive design standards in the green building system mainly aim at maximizing the improvement of indoor environmental performance and building energy efficiency. Building layout, building envelope, geometric form, material properties, and infiltration & airtightness are all identified as key factors for the passive design of buildings in hot and humid climates (Chen et al.,2017). Sensitivity analysis (SA), dynamic building energy simulation optimization (BESO), and decision-making model by applying genetic algorithm (GA) for high-rise residential buildings (Chen & Yang, 2017) provide design guidelines for built environments under natural or mixed ventilation mode.

In previous studies, the application methods of passive strategies in architectural design have limitations, with step redundancy and repetition, lacking a certain paradigm and universality. To fill the gaps in the current studies, this paper aims to investigate the effectiveness and optimization strategies of passive design methods based on climate change adaptation. Its originality lies in the following aspects: (1) Redraw the dynamic Givoni bioclimatic chart (GBC) referred to the passive strategy assessment method of the psychrometric chart to guide for determining relevant passive design parameters; (2) Summarize and analyze characteristics of local high-rise residential buildings and benchmarks of energy consumption data, and analyze thermal modeling in BESO method; (3) Rank and compare simulation datasets by SA method, the dynamic effectivenesses of each parameter are discussed through diachronicity and synchronicity; (4) Select the passive design parameters for GA optimization and decision-making, define the optimal passive design solution. In summary, the results of this study will provide a solid reference for the dynamic effectiveness and thermal performance optimization of the passive design of high-rise apartments in hot and humid regions.

2. Methodology

2.1 The framework of the study

This study attempts to propose passive design strategies for high-rise apartments in humid and hot regions adapting to climate change based on an integrated method in the BESO procedure, mainly focusing on a three-phase simulation optimization combined with sensitivity analysis. In this section, the datasets, reference indices, simulation tools, design parameters, and analysis and optimization methods used in the research are introduced. Specifically, the first step illustrates the dataset for future climate hours, and the generation and computation of dynamic GBC for the

selection of passive strategies; The second step is the building performance simulation setup by incorporating reference criteria for energy and comfort models; The third step introduces the Morris screening method in global SA to identify the importance and correlation between multiple input parameters and multiple objectives; The fourth step validates the feasibility of the decision-making process and solution by employing the NSGA-II model to provide Pareto optimal solutions for BESO. The methodological framework is shown in Fig. 1.

Figure 1: Methodological framework of the study

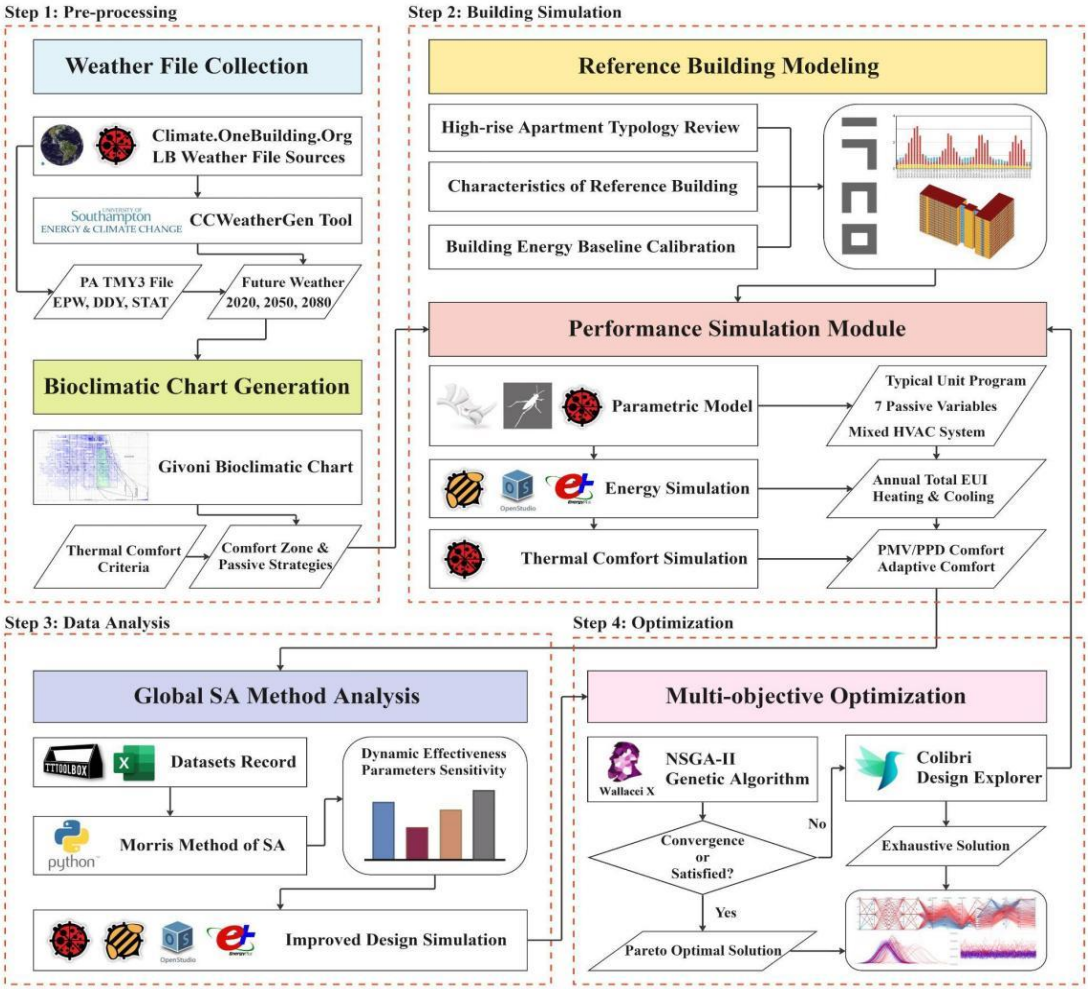

Source: Authors

2.2 Future weather dataset

Until now, global climate models (GCMs) have been used to simulate future climate conditions, providing regional or global averages to assess the impact of climate change on building performance. GCM simulations are in the 100-300 km^2 range, and the temporal resolution is in months (Moazami et al.,2019). In this study, future weather data is estimated by CCWorldWeatherGen, which generates climatic variable files for building performance simulations based on Hadley Center Coupled Model Version 3 (HadCM3) and IPCC A2 emissions

scenarios, representing short-, medium-, and long-term scenarios. The generated data is consistent with the local climatic circumstances of the study.

2.3 Reference building features and baseline model

2.3.1 Typical High-rise apartment archetypes

From the 1960s to 1970s, high-rise affordable housing emerged in densely populated cities in the Northeast region of the United States, including Philadelphia. For example, the collective dormitory featured multi-unit and single-aspect with double-loaded corridors (Yanni, 2019). However, these aging buildings face thermal performance issues due to poor insulation, low airtightness, lack of shading devices and inadequate natural ventilation, which pose risks of indoor overheating and extreme cold. This study focuses on three representative high-rise apartments in University City, with Sansom Place West (SPW) as the primary subject for simulation, analysis, and optimization. The basic information of the three buildings is shown in Tab. 1 and Fig. 2.

2.3.2 Baseline simulation model setting

The study adopts a cross-platform tool of Openstudio based on the EnergyPlus simulation engine to set parameters and calibrate baselines of the building, which allows for the simulation of building performance and thermal comfort under different climate scenarios. The thermal model focuses on the middle typical floor plan (Fig. 3), dividing it into different zones based on unit type and program. The residential density of the building is approximately 0.05 people/m², the HVAC system is a DOAS (dedicated outdoor air system), and the simulation employs a changeover mixed-mode strategy to control the window opening time. The energy consumption report (2018) of SPW summarize in Tab. 2 and the data of the building are listed in Tab. 3. Considering factors such as the periodic transitions of the real building, the data results of the ideal model closely align with the actual conditions.

Table 1: Basic information of selected high-rise apartments in Philadelphia

No.	Name	Location	Year Built	Building Type	Number of Floors	Floor Area (m2)	Building Height (m)	Type of Unit (pers.)	Layout Pattern	Passive System
1	Sansom Place West	Chestnut St, PA	1970	On-campus Apartment	16	1140	48	1/2/3	L-shaped	No Shading; Less Ventilation; Bad Insulation
2	Sansom Place East	Chestnut St, PA	1970	Commercial Apartment	16-23	1090	69	1/2	Z-shaped	No Shading; Less Ventilation; Bad Insulation
3	Mason on Chestnut	Chestnut St, PA	1970	International Apartment	15	1060	45	1	I-shaped	Shading; Natural Ventilation; Buffer Zone

Source: Authors

Figure 2: The location of building samples and abstraction of building footprint archetypes

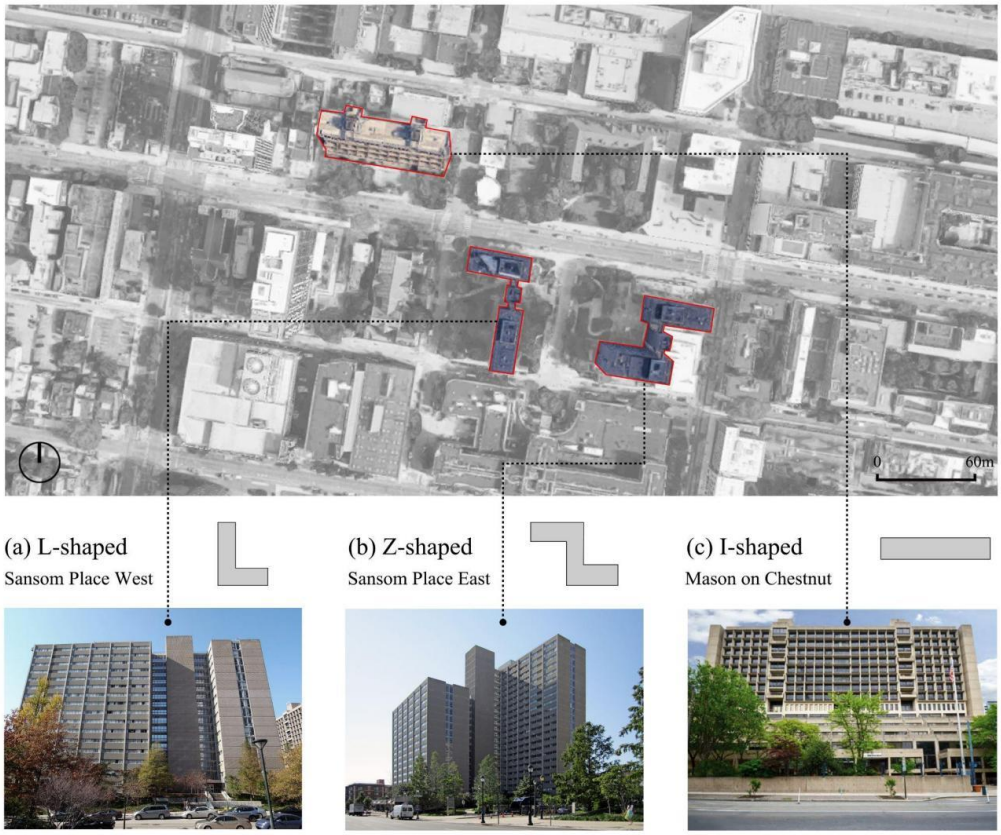

Source: Authors

Figure 3: Typical floor plan (a), the whole building model (b), four types of room unit (c), and simulation thermal model (d) of Sansom Place West in Philadelphia

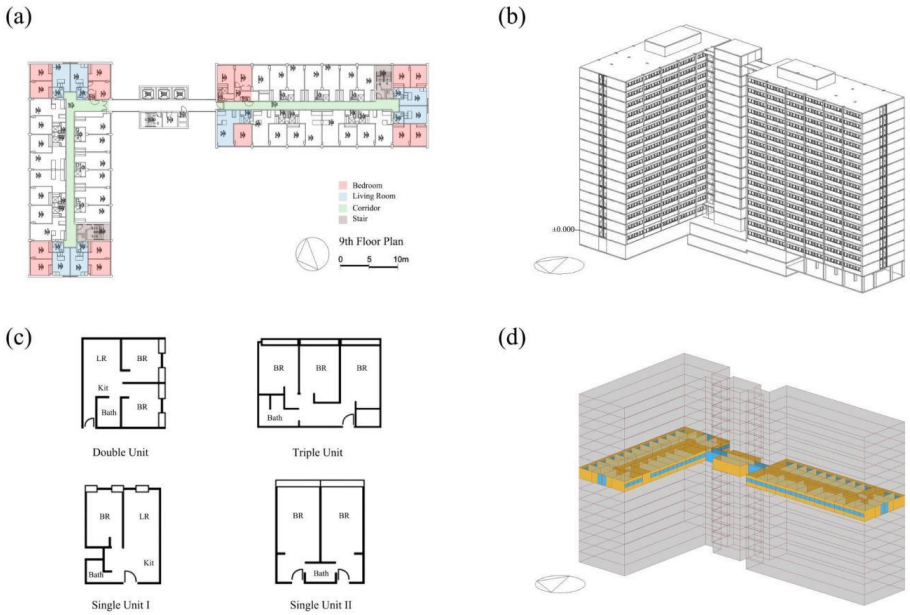

Source: Authors

Table 2: Annual building energy consumption of Sansom Place West in FY2018

Building Energy Consumption	Source	Units	kWh	kWh/m^2
Electricity	973,371	kWh	873,202.36	40.4
Steam	8,767	mlb	3,109,712.26	143.5
Chilled Water	1,282,087	kBtu	375,670.12	17.3
Total			4,358,584.74	201.2

Source: Authors

Table 3: Building parameters and baseline simulation results of thermal modeling

Parameter	Unit	Value
Window U-factor	W/m^2-K	3.5
Window Solar Heat Gain Coefficient	-	0.6
Wall R-value	m^2-K/W	2
Window Open Area Ratio	%	10
Window-to-Wall Ratio of Bedroom	%	40
Window-to-Wall Ratio of Living Room	%	90
Wall Solar Absorptance	-	0.7
Solar Protection	m	0
Net Storey Height	m	2.6
Occupant Density	people/m^2	0.05
Annual EUI	kWh/m^2	262.25
Heating Load	kWh/m^2	114.26
Cooling Load	kWh/m^2	65.94
PMV Comfort (Conditioned)	%	38.71
Adaptive Comfort (Unconditioned)	%	19.01

Source: Authors

2.3.3 Thermal criteria of passive survivability

Generally, the cooling strategy for residential buildings involves a mixed-mode approach. This study refers to ASHARE 55 and adopts the predicted mean vote (PMV) model and adaptive comfort standard (ACS) model. Passive survivability[1] requires defining the habitability zone for safe conditions during power outages, which has a broader temperature threshold than the comfort zone. LEED and RELi Rating System provide three compliance paths for demonstrating passive

[1] A new climate adaptation design standard in the U.S. building industry, refers to the idea that certain buildings, especially houses and apartment buildings, should be designed and built to maintain habitable temperatures in the event of an extended power outage or interruption in heating fuel (Wilson, 2006).

survivability, which include the standard effective temperature (SET), psychrometric analysis, and passive house certification.

The study uses the psychrometric compliance path, considering metrics like WBGT and heat index to determine temperature thresholds. In summer, indoor conditions should not exceed the extreme caution in metrics, that is, dry bulb temperature (DBT) below 32°C and WBGT below 28°C. In winter, DBT should be above 10°C. The relationship function is as follows:

$$WBGT_{indoor} = (0.7 * T_w) + (0.3 * T_g) \quad (1)$$

$$\begin{aligned} T_w = T * \arctan\left[0.151977 * (RH\% + 8.313659)^{\frac{1}{2}}\right] \\ + \arctan(T + RH\%) - \arctan(RH\% - 1.676331) \\ + 0.00391838 * (RH\%)^{\frac{3}{2}} \\ * \arctan(0.023101 * RH\%) - 4.686035 \end{aligned} \quad (2)$$

where

T= Dry Bulb Temperature in Celsius

Tw = Wet Bulb Temperature in Celsius

Tg = Globe Thermometer Temperature in Celsius

RH% = Relative Humidity

2.4 Bioclimatic chart and passive strategies

2.4.1 Givoni Bioclimatic chart

The GBC (Fig. 4a) is widely used in architectural practice and research, divides regions and suggests specific passive design strategies to improve indoor thermal comfort (Morillón-Gálvez et al., 2004), (Manzano-Agugliaro et al., 2015). Building retrofit based on passive design effectively addresses climate change and enhances building adaptation, but the energy efficiency effects vary across different climate scenarios. This study establishes cooling and heating strategies based on GBC and other charts (Fig.4b, Fig.4c), and develops a customized GBC for Philadelphia's climate (Fig. 5).

Figure 4: Primary Milne-Givoni bioclimatic chart (a), Milne-Givoni bioclimatic chart redrawn by DeKay and Brown (b), and revised Milne-Givoni bioclimatic chart redrawn by Roshan et al.

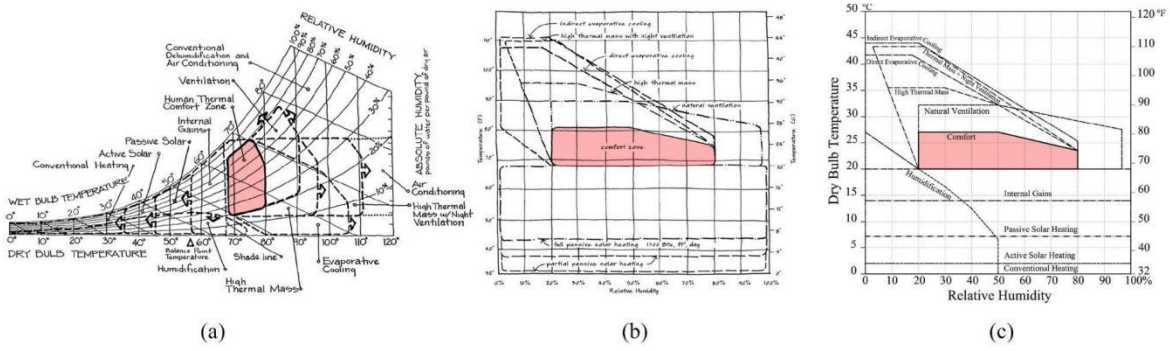

Source: Watson, D. (1993) (a), DeKay , M. & Brown, G. (2014) (b), Roshan, Gh. R. et al. (2017) (c)

Figure 5: Horizontal Givoni bioclimatic chart drawn by authors

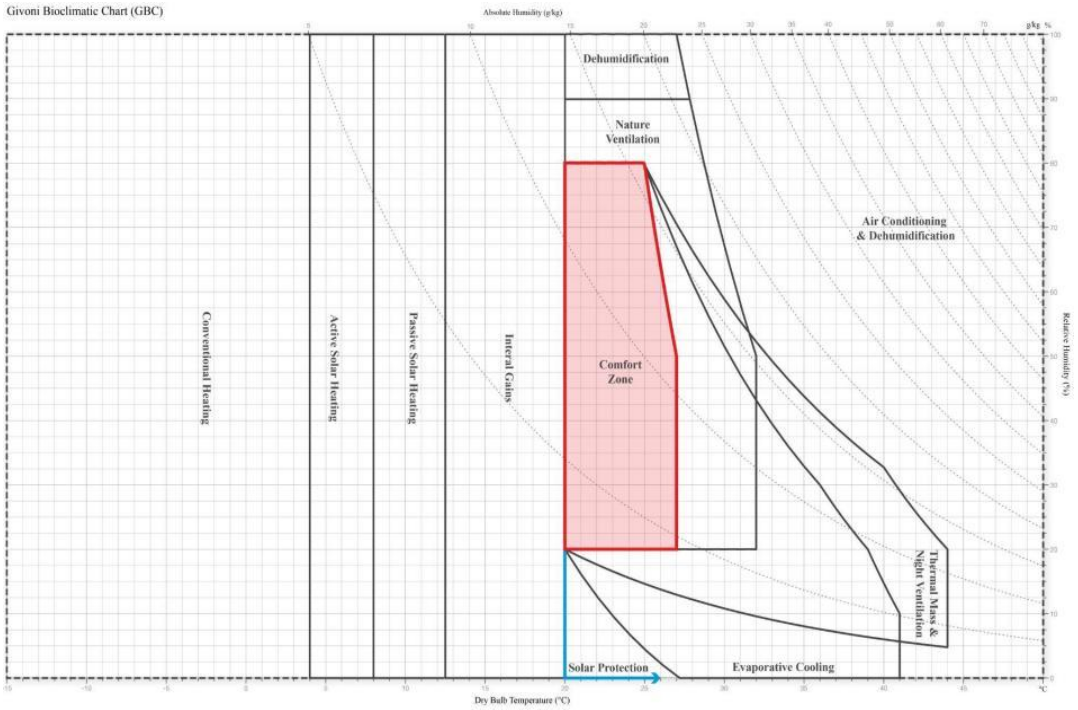

Source: Authors

2.4.2 The variables of passive design

To validate the effectiveness of passive design strategies by providing detailed descriptions of key building physical parameters for SPW, the variables include the building's opaque envelope, fenestrations and glazing material, shadings, and airtightness (Ferrara et al., 2014), (Asadi et al., 2012). The details are as follows:

(1) Opaque envelope: The performance of the external walls is particularly crucial for building energy efficiency and indoor thermal comfort and the building envelope of SPW does not provide effective thermal insulation and insulation, considering R-value and wall solar absorptance (WSA) as parameters.

(2) Fenestrations and glazing material: SPW with large window areas, low-performance glass, and lack of cross ventilation do not provide adequate thermal comfort but only ensure a certain level of daylight quality. Parameters related to window properties, such as U-factor, SHGC, WWR, and window open area ratio (WOAR) for natural ventilation cooling, are included.

(3) Shadings: No additional shading devices combined with large open windows and low-performance glass, the issue of indoor overheating in hot climates cannot effectively mitigate, focusing on the dynamic impact and scheduling strategies of the shading system on the various room orientations.

(4) Airtightness: In this study, the airtightness of high-rise residential buildings is addressed, assuming that existing airtightness can be improved from "very poor" to "excellent" through caulking techniques. Infiltration values used in thermal modeling range from 0.001 to 0.0006,

indicating typical crack flow coefficients and exponents for different envelope tightness classifications.

In summary, Tab. 4 shows the units and specific ranges of the important parameters in passive design strategies.

Table 4: Building design parameters and their ranges under uniform distribution for sensitivity analysis and multi-objective optimization

No.	Parameter	Abbreviation	Unit	Range
1	Window U-factor	WinU	W/m^2-K	0.30-5.90
2	Window Solar Heat Gain Coefficient	SHGC	-	0.20-0.69
3	Wall R-value	WallR	m^2-K/W	1.68-4.48
4	Window Open Area Ratio	WOAR	%	10-80
5	Window-to-Wall Ratio of Bedroom	WWRB	%	20-55
6	Window-to-Wall Ratio of Living Room	WWRL	%	34-90
7	Wall Solar Absorptance	WSA	-	0.10-0.73

Source: Authors

2.5 Sensitivity analysis method

This study adopts the Morris method, a global screening method, to evaluate design parameters efficiently and rank their influence. Python is used for data processing, modeling analysis, and result visualization. Only one input parameter is assigned a new value in each subsequent run in Morris Method (Saltelli et al., 2004), commonly known as a trajectory or elementary effect (EE), and a group of trajectories enables statistical evaluation of finite distributions of EE (Menberg et al., 2016). The sampling of the input parameters uses a predetermined probability distribution function to realize the individual perturbation of the parameters (Pang et al., 2020), (Cao et al., 2022). Fig. 6 presents the Morris sampling method of SA and the schematic diagram of the output results.

Figure 6: Morris sensitivity analysis method based on trajectory, and its schematic diagram with absolute average (μ) and standard deviation (σ)*

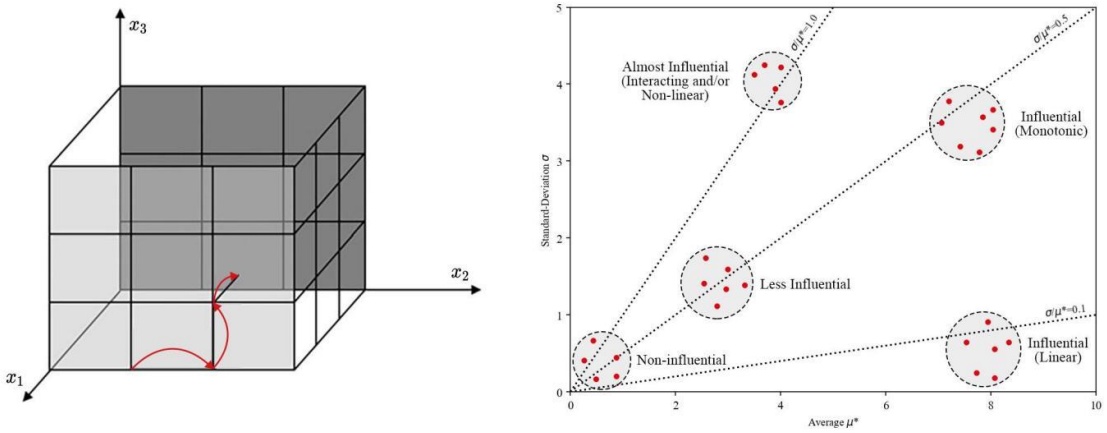

Source: Authors

Set the range of K input parameters before calculation and specify i values within the range of variation (Morris, 1991). The EE for each input variable k is defined as:

$$EE_k = \frac{Y(x_1, x_2, \dots, x_k + \Delta, \dots, x_K) - Y(x_1, x_2, \dots, x_K)}{\Delta} \quad (3)$$

where Y is the output variable, vector X represents K parameters[2], and the kth parameter needs a grid jump Δ.

Common statistical measures used to evaluate EE include mean μ and standard deviation σ:

$$\mu_k = \frac{1}{nR} \sum_{r=1}^{nR} EE_k^r \quad (4)$$

$$\sigma_k = \sqrt{\frac{1}{nR} \sum_{r=1}^{nR} (EE_k^r - \mu_k)^2} \quad (5)$$

Where r is the serial number of the sampling trajectories group where the current input variable k locates, and nR is the total number of sampling trajectories.

To circumvent the problem that changes in parameter values lead to canceling effects, the equation of μ^* is defined as:

$$\mu_k^* = \frac{1}{nR} \sum_{r=1}^{nR} |EE_k^r| \quad (6)$$

In the equations, μ^* represents the sensitivity of the parameter, the larger the value, the stronger the sensitivity of the parameter; σ represents the strength of the nonlinear effect or interaction between parameters, the higher the value, the stronger the parameter interaction is. The results of the Morris screening method can be represented by a scatter diagram (Liu et al., 2020). Referring to the ratio of σ to μ^*, the impact of the parameters is monotonic when $0.1<\sigma/\mu^*<0.5$, detailed in Fig. 6.

Through the review of the SA method, when the i value ranges from 4 to 10 (Heiselberg et al., 2009), and the change trajectory ranges from 10 to 50 (Ruano et al., 2012), it can guarantee sufficient sample size and reduce the calculation cost to the greatest extent. This study set each parameter to 8 elementary effects based on 4 weather scenarios, and the total change trajectories were set to 40 (Campolongo et al., 2007). Therefore, the total number of simulations is 1280, and there are 5 output values in total, namely EUI, PMV Comfort, Adaptive Comfort, Heating, and Cooling. Analysis and selection of critical design parameters for later optimization and verification will be facilitated with the use of the results of the Morris SA method.

2.6 Multi-objective optimization method

NSGA-II algorithm (Fig. 7) increases solution diversity while adhering to constraints (Wang et al., 2021). The BESO model incorporates significant parameters identified by the Morris SA method for multi-objective optimization. WallaceiX plug-in, integrated with NSGA-II, enables rapid evaluation and visual multi-objective optimization through proxy models in Grasshopper, aiding

[2] The input data $X= (x_1,x_2... ,x_K)$ must be normalized to ensure that the calculation result of the sensitivity is not affected by the unit change of input value in the practical application scenario.

in selecting optimal parameter combinations for passive design strategies (Huang et al., 2022). Additionally, the Colibri plug-in and Design Explorer are employed to obtain optimal solutions for specific rooms, considering nonlinear design parameters.

Figure 7: The flow diagram of the NSGA-II algorithm

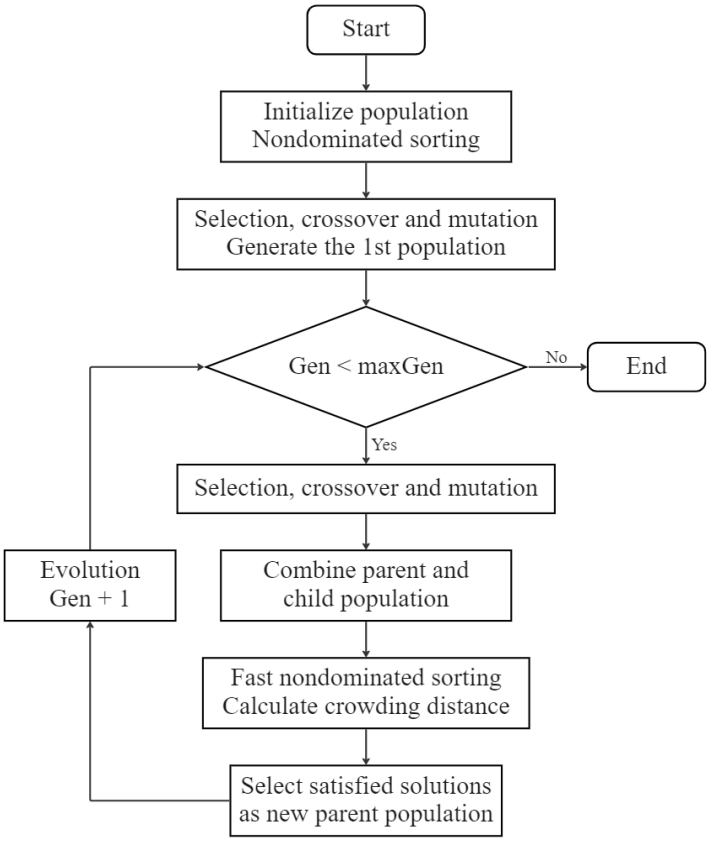

Source: Authors

3. Results

3.1 Dynamic trends of passive strategies in GBC

The study utilized future data based on EPW files to investigate passive strategies under different climate scenarios. The GBC plots from the EPW of TMY to 2080 scenarios are plotted in Fig. 8, indicating the dynamic hours and importance of passive design strategies represented by the color blocks in different regions. Overall, the color blocks shift towards the right end of the GBC over time. This signifies that the indoor thermal environment in the regions will inevitably face increasingly hotter and more humid conditions due to climate change. Consequently, buildings will require higher energy consumption to cope with climate change, and there will be higher demands on building performance to ensure thermal comfort for occupants.

In terms of time data of GBC, there is a relatively small fluctuation in the climate comfort zone throughout the 21st century, decreasing from 1035 hours under TMY (Fig. 8a) to 937 hours under 2080 (Fig. 8d). The result may be attributed to the warming of the subtropical region, which weakens the need for primary heating strategies during the winter season. For instance, the internal gain decreases from 1920 hours in TMY to 1700 hours in 2080, and conventional heating is

significantly reduced from 2154 hours in TMY to 1118 hours in 2080, which is almost halved. While the relatively small change in solar heating is due to the small effect of solar radiation.

Figure 8: Givoni bioclimatic charts of Philadelphia under four different climate scenarios: TMY (a), 2000 (b), 2050 (c), and 2080 (d)

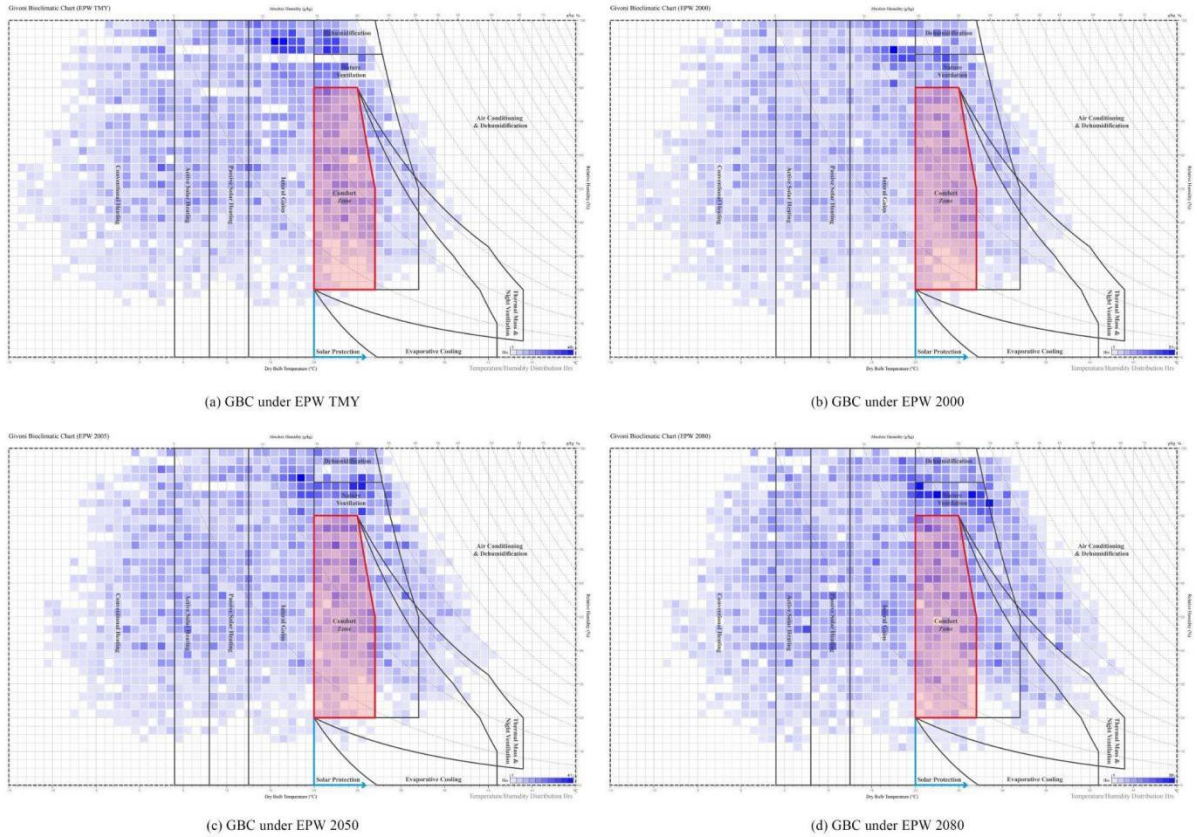

(a) GBC under EPW TMY

(b) GBC under EPW 2000

(c) GBC under EPW 2050

(d) GBC under EPW 2080

Source: Authors

Figure 9: The number of hours for heating and cooling strategies in four climate scenarios

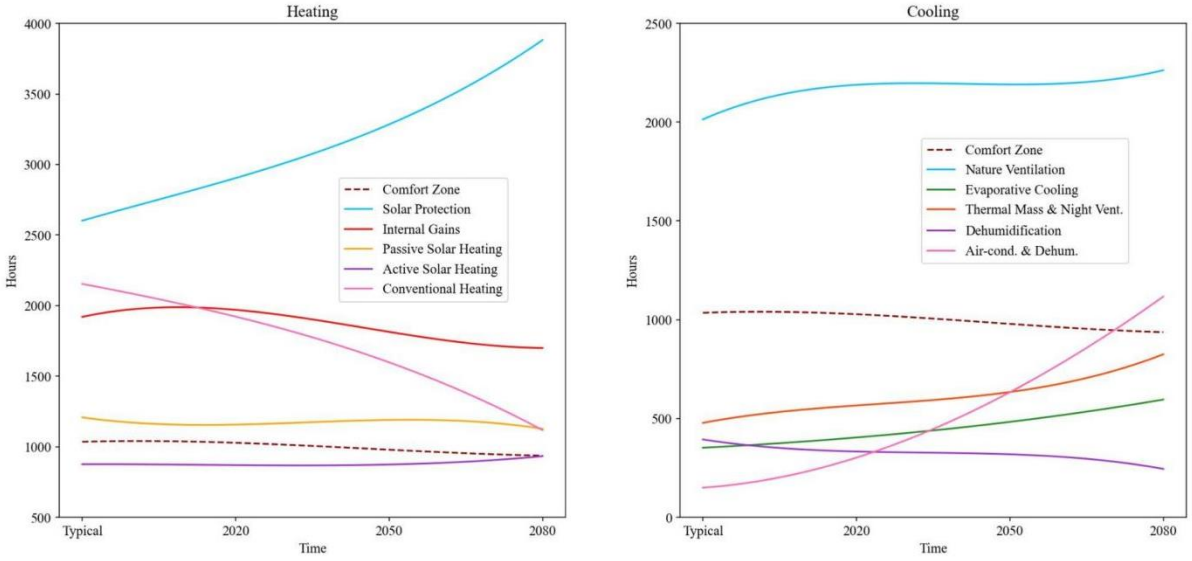

Source: Authors

When examining the variations in the duration of cooling strategies under different climatic scenarios (Fig. 9) most passive cooling strategies do not exhibit a significant upward dynamic trend. Especially in hot and humid environments, natural ventilation and dehumidification fail to address thermal comfort issues effectively. The combined duration of these strategies transitions from 2408 hours in the TMY to 2508 hours in 2080, accounting for nearly the same proportion of the total annual hours. The results indicate that only solar protection directly reflects a strong dynamic increase for shading and radiation control in the future, nearly doubling its effectiveness. And the building envelope attributes such as windows and walls will continue to have a relatively effective impact. Furthermore, there is a significant increase in the demand for air conditioning with dehumidification in buildings, indicating the growing importance of mechanical systems in mitigating overheating conditions. The duration of air conditioning with dehumidification strategies increases from 150 hours in the TMY to 1116 hours in 2080.

3.2 Sensitivity evaluation of passive design parameters

This study plotted a radar chart (Fig. 10) based on building energy consumption and thermal comfort as the overall sensitivity objectives. By comparing them chronologically, the dynamic changes in the sensitivity of each parameter to the objective values can be observed. Taking the output results of EUI as an example, the sensitivity of WSA and SHGC significantly increases over the years, with an expected increase of 235% and 152% by the 2080s. This indicates that the solar heat gain coefficient on the building envelope has an increasingly significant impact on future building energy consumption. Additionally, the μ^* of WWRB increase from 23.51 to 29.60, WinU decreases from 38.35 to 32.35 and WallR decreases from 25.95 to 23.30, while WOAR and WWRL show lower sensitivity. Meanwhile, SHGC and WSA exhibit contrasting μ^* in heating and cooling loads, reflecting their influence on the heating and cooling demands based on the solar heat gain coefficient on the building envelope. In comparison, the μ^* values of parameters related to human thermal comfort are relatively small. Among them, SHGC shows the largest sensitivity change in PMV model, increasing by 298%, while WallR exhibits the largest sensitivity change in Adaptive model, increasing by 41%.

The sensitivity of passive design parameters is comprehensively ranked, and their timeliness and importance trends are evaluated using a heat map (Fig. 11). Through the analysis of heating and cooling targets in building energy consumption, SHGC and WWRB have significant dynamic impacts and become important design considerations for the future. WSA is relatively important in hot conditions, while WinU and WallR are more important in other conditions, and both exhibit stable trends. Additionally, in the thermal comfort model, the importance of WallR and WinU also significantly increases in the future. On the other hand, WOAR shows a clear decreasing trend across multiple target values, indicating a decline in the dynamic effectiveness of natural ventilation through window opening over time.

Moreover, the range definition of the SA schematic diagram demonstrates that when the σ/μ^* of the parameter is between 0.1 and 0.5 in the scatter plot, the parameter exhibits both monotonicity and a certain level of influence. This study mainly selects climate scenarios of TMY and 2080 to identify the distribution of σ/μ^* for the corresponding parameters of each target output. In the TMY plot (Fig. 12a), the σ/μ^* of WinU, WallR, and SHGC are generally between 0.1 and 0.5, showing a linear and significant impact on building energy consumption. For Cooling, the σ/μ^* of WinU and WallR exhibit a special case with $\sigma/\mu^* > 1$, indicating that buildings with highly insulated windows and walls may not perform well in hot conditions. However, the σ/μ^* of WOAR is

between 0.1 and 0.5, suggesting that natural ventilation remains effective in current conditions. On the other hand, in the 2080 plot (Fig. 12b), the σ/μ^* of WinU, SHGC, WallR, WWRB, and WSA are generally between 0.1 and 0.5, especially for cooling, gradually exhibiting a unified monotonic trend. This shows that optimizing the thermal properties of windows and walls is more effective in building performance under future climate change. Additionally, based on the thermal comfort model, WinU shows an almost monotonic trend, with σ/μ^* close to 0.5 and on the outer side, indicating the significant impact of window performance and area on thermal comfort in the future.

Figure 10: The radar chart of μ^* of parameters in four climate scenarios

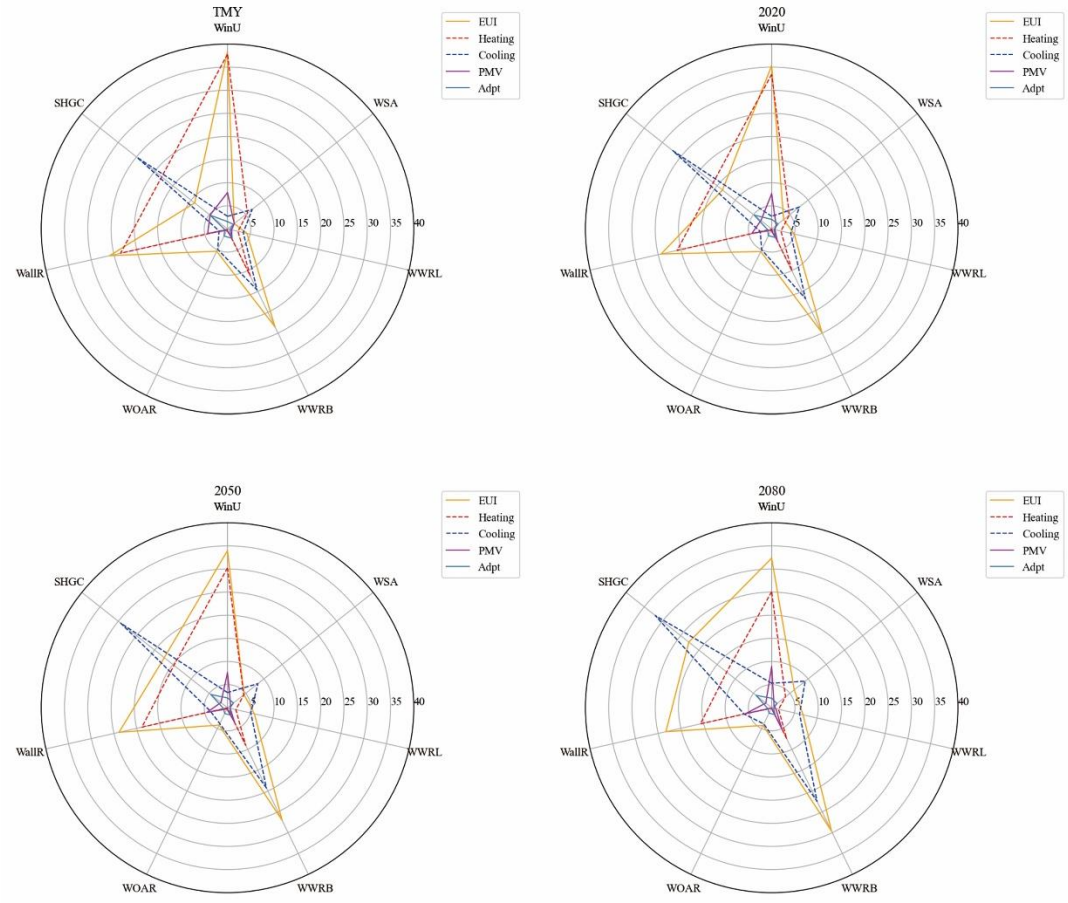

Source: Authors

Figure 11: The heat map of sensitivity ranks of passive design parameters

Objective	EUI				Heating				Cooling				PMV Comfort				Adaptive Comfort			
EPW	TMY	2020	2050	2080	TMY	2020	2050	2080	TMY	2020	2050	2080	TMY	2020	2050	2080	TMY	2020	2050	2080
WinU	1	1	1	1	1	1	1	1	6	6	7	6	1	1	1	1	5	2	2	2
SHGC	4	4	4	4	3	3	3	3	1	1	1	1	2	3	4	4	1	1	1	1
WallR	2	3	3	3	2	2	2	2	7	7	6	5	3	2	2	2	6	6	6	6
WOAR	5	5	7	7	7	7	7	7	4	4	5	7	7	7	7	7	3	5	5	5
WWRB	3	2	2	2	4	4	4	4	2	2	2	2	4	4	3	3	2	3	3	3
WWRL	6	6	5	5	6	6	6	6	5	5	4	4	6	6	6	5	7	7	7	7
WSA	7	7	6	6	5	5	5	5	3	3	3	3	5	5	5	6	4	4	4	4

Most Sensitive — Ranking Legend — Least Sensitive

1 2 3 4 5 6 7

Source: Authors

Figure 12: The scatter plot of σ/μ of parameters for climate scenario of TMY and 2080*

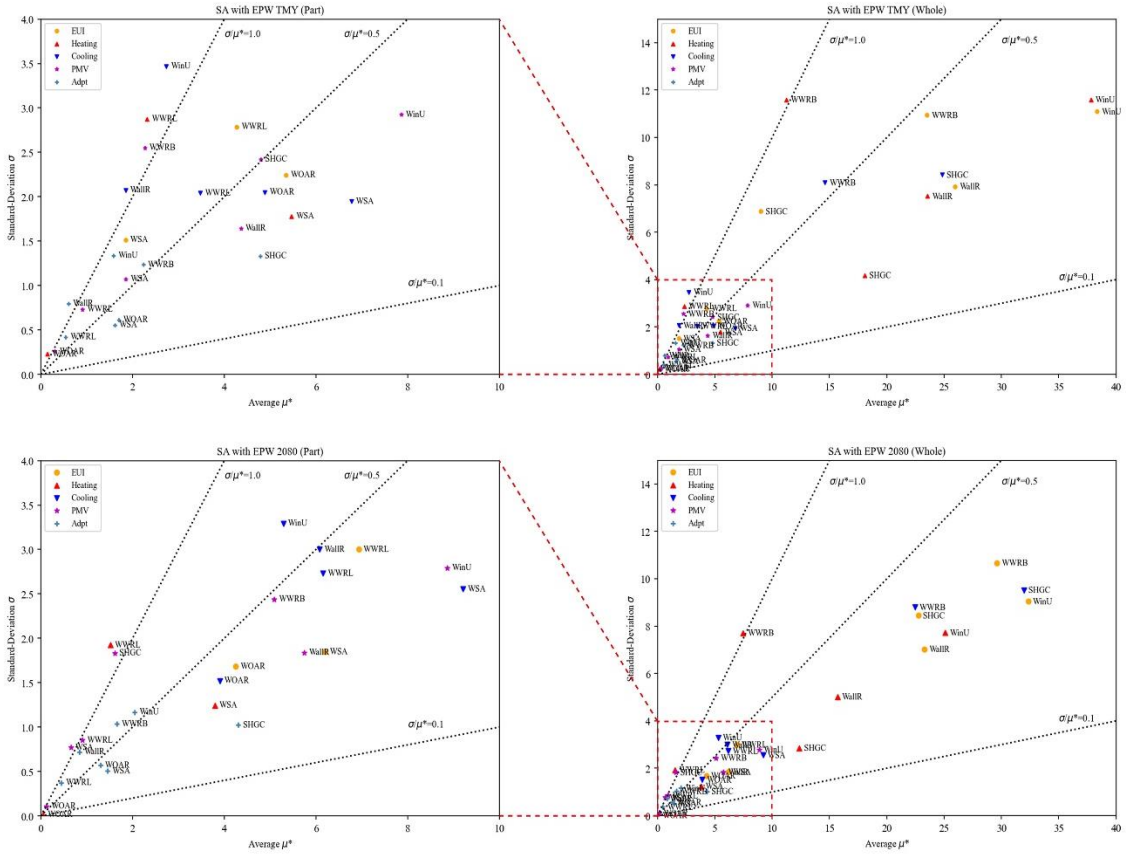

Source: Authors

3.3 Optimization and decision-making by generation algorithm

This study summarizes the dynamic analysis of the parameters based on the aforementioned charts to demonstrate the timeliness of using passive design parameter combinations for building energy efficiency and thermal comfort under different climatic scenarios. Multi-objective optimization selects the main variables in the optimization model based on parameters that rank high in sensitivity or exhibit significant and monotonic. For the TMY scenario, this study selects WinU, WallR, SHGC, and WOAR as the optimization parameters. For the 2080 scenario, WinU, WallR, SHGC, WSA, and WWRB are chosen as the future optimization parameters to adapt to the trend of hot and humid climate change.

The multi-objective optimization results of NSGA-II yield a Pareto front solution, representing the optimal solution space. In this study, the WallaceiX plugin was used to set quantitative generation size and count for crossover and mutation, conducting BESO in Grasshopper for both typical and late 21st-century climate scenarios. The simulation results of the optimized Annual EUI and PMV Comfort are shown in Fig. 13, wherein the normal distribution functions for both climate scenarios exhibit a significant leftward shift and gradual convergence. Additionally, the parallel coordinate plot (Fig. 14) demonstrates a tendency for the four fitness values to converge downwards after iterations. These observations indicate that the results of the genetic algorithm align with the expected optimization outcomes.

Figure 13: Standard deviation of fitness values for the climate scenario of TMY and 2080

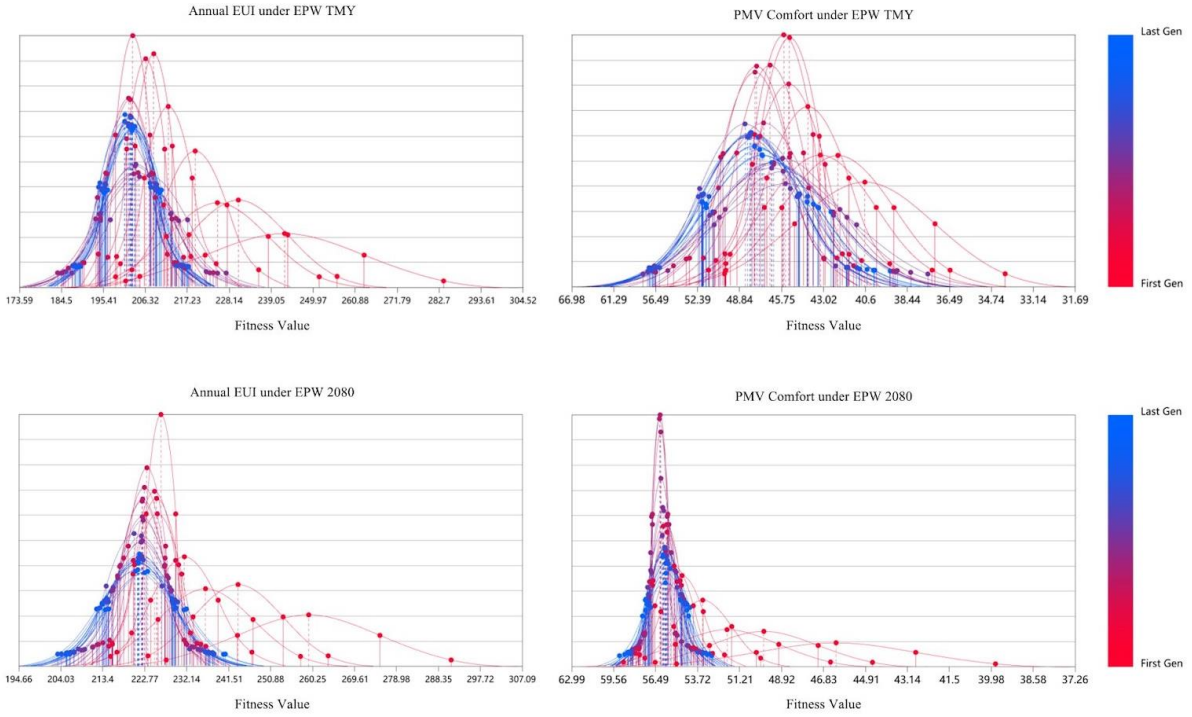

Source: Authors

Figure 14: Parallel coordinate plot and diamond fitness chart for the climate scenario of TMY and 2080

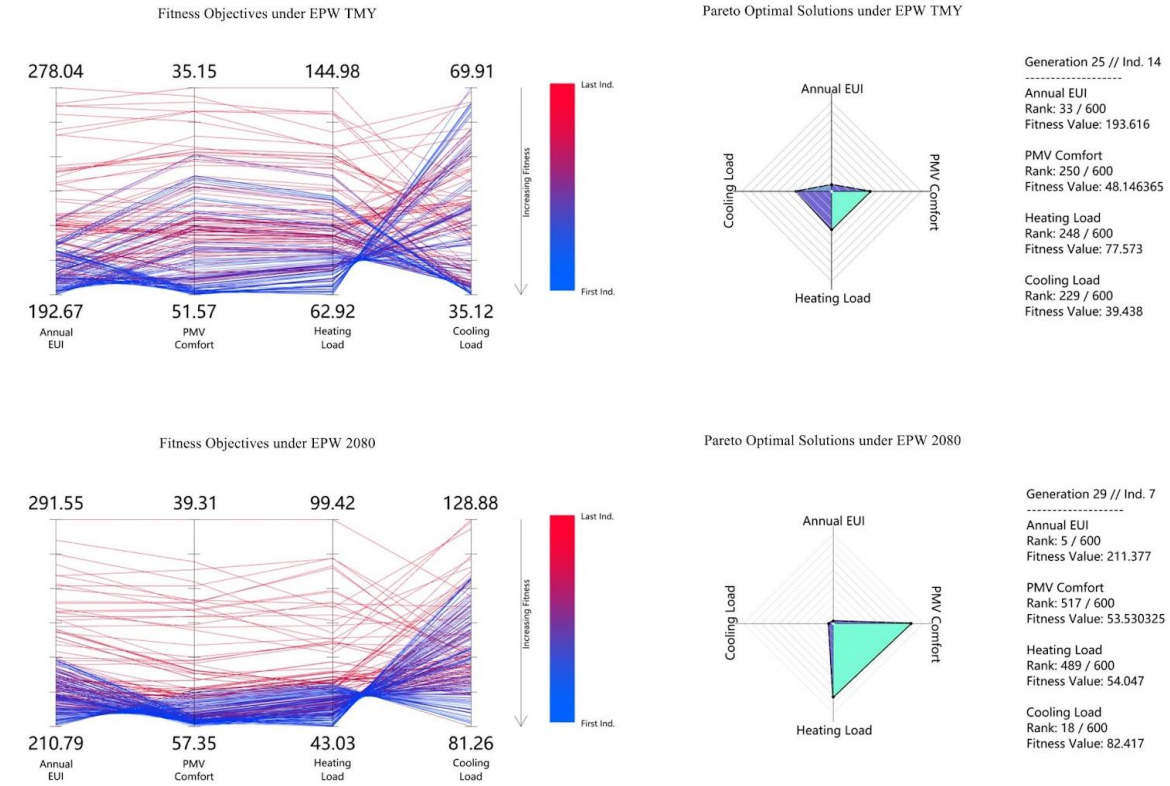

Source: Authors

To compare the final effects of fitness values under current and future climate change scenarios, the Pareto front solutions from the last few generations of the GA were selected. The distribution frequencies of the four genetic variable parameters within a unified range were analyzed (Fig. 15). By comparing the optimized parameters for the two climate scenarios, it was found that achieving the optimal values is possible when WinU is smaller, WallR is larger, and SHGC gradually decreases over time. Improving WOAR is particularly important for the current climate while reducing WWR is necessary for the future to minimize heat gain. Moreover, based on the selection of the highest scores of the "average of fitness ranks" in Fig. 14, an exhaustive optimization was conducted in Design Explorer. Specifically, the variables of shade depth and count were chosen, considering the room's airtightness to reduce the impact of high-humidity hot climates on building insulation. In the TMY scenario, it was found through sensitivity analysis that WWRB exhibits nonlinear and significant characteristics, thus it was included in this optimization process. In conclusion, the specific retrofit measures and the comparison of simulation results are shown in Tab. 5.

Figure 15: Distribution frequency of four genes in all Pareto front solutions

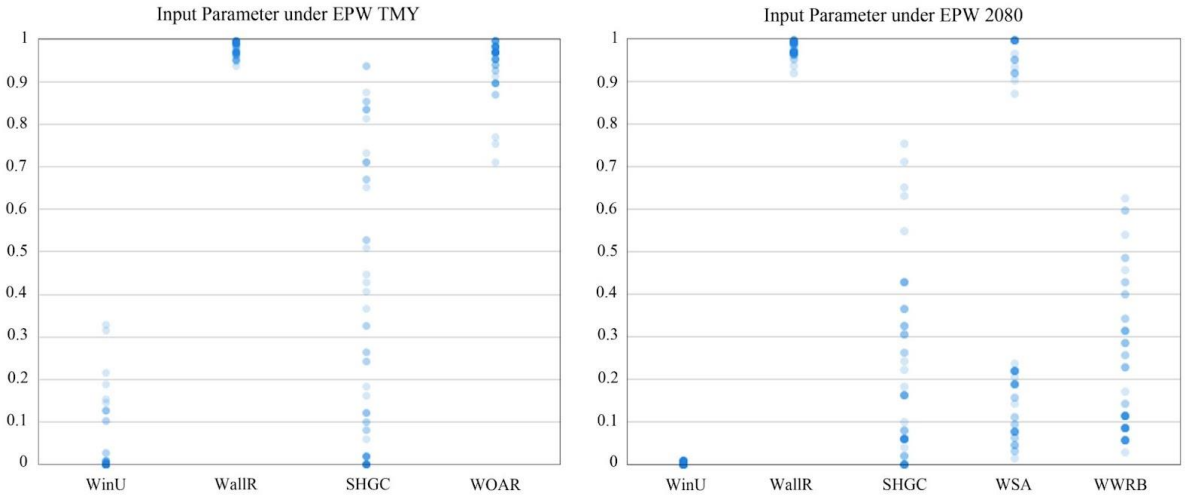

Source: Authors

Table 5: Passive design methods of retrofit strategy under the climate scenario of TMY and 2080

Climate Scenario	Opaque Envelope	Fenestration with Glazing	Shading and Opening	Airtightness
Retrofit Strategy in TMY	Replace external tiles and insulation panel (WallR=4.4)	Replace single clear glass to Low-e glass (WinU=0.3; SHGC=0.25)	Adding 0.5m overhang shading with louvers; Improve window open area ratio to 78%	Keep average infiltration air flow intensity to 0.0003
Retrofit Strategy in 2080	Replace external tiles and insulation panel (WallR=4.4; WSA=0.14)	Replace single clear glass to Low-e glass (WinU=0.31; SHGC=0.2)	Adding 0.5m overhang shading with louvers; reduce WWR of bedroom to 0.25	Keep average infiltration air flow intensity to 0.0003

Results	Annual EUI	Heating Load	Cooling Load	PMV Comfort
Retrofit Strategy in TMY	153.6	42.25	31.08	50.37
Retrofit Strategy in 2080	171.62	31.46	67.69	58.54

Source: Authors

4. Discussion

4.1 Application of optimization result on the residential buildings

After the final optimization, the simulated results exhibit significant changes compared to the baseline. In the TMY scenario, the EUI is reduced by 41.4%, with Heating decreasing by 60.4%, Cooling decreasing by 52.9%, and PMV increasing by 30.1%. In the 2080 scenario, the EUI is reduced by 40.5%, with Heating decreasing by 56.6%, Cooling decreasing by 49.5%, and PMV increasing by 40.5%. Under the trend of high temperature and high humidity climate change in the future, the performance requirements for buildings increase. However, optimization through passive design can significantly mitigate energy consumption and improve the passive survivability of buildings. The simulation comparison and temperature statistics during power outages show that the interior DBT threshold (10℃-32℃) increases by 431 hours in the TMY scenario (from 5,745 hours to 6,176 hours) and by 561 hours in the 2080 scenario (from 5,221 hours to 5,782 hours).

4.2 Key findings on SA method and GA simulation

According to the results obtained through the SA method, it is possible to intuitively obtain parameter characteristics such as monotonicity, influence degree, and sensitivity. However, it is not possible to accurately determine the positive correlation between parameters and their impact on results, nor can it directly determine the optimal parameter values. On the other hand, utilizing the Pareto optimal solution space obtained through GA allows for the selection of combination logic and objective ranking among various parameters, which is an effective means to aid optimization. Furthermore, since this study ultimately aims to optimize multiple objectives, parameter selection cannot solely rely on common sense judgment. Therefore, combining SA and GA can greatly enhance the efficiency and extent of the simulation process.

In this study, the NSGA-II algorithm was utilized for optimization with a configuration of 30 generations and 20 individuals per generation, which is significantly fewer than the conventional benchmark of 5,000 genes. The primary reason for this choice is based on the σ/μ^* analysis of parameters obtained through SA, enabling the combination of monotonic parameters within a limited cluster to rapidly search for the optimal solution space, thereby enhancing simulation efficiency and reducing computational time. The fitness function exhibits consistent changes rather than fluctuations, allowing effective results to be obtained through the selection of combined sensitivity parameters within a smaller number of simulation iterations. Further analysis of relevant parameters using exhaustive methods refines the results under different climatic scenarios, facilitating the dynamic effectiveness of the passive design.

4.3 Limitations of effectiveness and optimization

During the research process, technical challenges related to the accuracy and reliability of generating future climate data are impossible to precisely predict the specific trends of global warming solely based on historical climate databases. Therefore, this study is limited to exploring the building environment based on typical weather file data. Additionally, tools such as BBG, SA, and GA cannot precisely measure the effectiveness of specific parameter combinations in passive design strategies. They mainly seek optimal data solutions through simulation optimization, often overlooking the impact of local microclimates, urban heat islands, disasters, vegetation distribution, and building form on energy consumption and thermal comfort. Nevertheless, through the current analysis of trends in typical high-temperature and high-humidity climate change in the subtropical region and comprehensive data modeling of existing buildings, specific methods for utilizing dynamic passive design to adapt to HSCW conditions in Philadelphia can be summarized. Furthermore, considering the resilience of different urban forms and climate adaptation of buildings may enhance the significance of this research and contribute to paradigmatic transformations in the retrofitting of apartments in subtropical regions.

5. Conclusion

The research results demonstrate that buildings in future high-temperature and high-humidity climates will face overheating issues. The significant increase in cooling load implies that buildings need to employ comprehensive passive design strategies to maximize insulation, thermal comfort, and energy efficiency. For different climatic environments, the use of large window areas to enhance natural ventilation remains effective in the current TMY climate, offering benefits such as dehumidification and increased daylighting. Simply improving the window-to-wall thermal resistance can substantially enhance thermal comfort, increasing it from 38.7% to over 50% throughout the year. Simultaneously, there is a significant reduction in the overall building energy consumption, by 109 kWh/m². Thus, efficient optimization can be achieved through material improvements to the facades of high-rise apartments in the present context. However, in simulations for the end of this century, the effectiveness of window ventilation diminishes, while solar protection and the WWR become dominant factors. By incorporating larger and operable shading devices and highly thermally resistant envelope structures, the threshold for passive survivability under extreme climate conditions is increased by 561 hours, maximizing thermal comfort. Nevertheless, it should be noted that thermal comfort in buildings under future high temperatures (>32℃) cannot be effectively alleviated through passive retrofitting alone. Even with a significant annual reduction in cooling load of up to 67 kWh/m², additional energy-saving measures such as mechanical systems and renewable energy should be considered.

References

International energy agency. World Energy Outlook, (2012). *International Energy Agency–International Organization for Standardization (IEA–ISO), International Standards to develop and promote energy efficient and renewable energy sources.* Special ISO Focus—World Energy Congress (2012), pp. 5-10

Kottek, M., Grieser, J., Beck, C., Rudolf, B., and Rubel, F. (2006). World map of the Köppen-Geiger climate classification updated. *Meteorologische Zeitschrift*, vol. 15(3), pp. 259–263. Available: https://doi.org/10.1127/0941-2948/2006/0130

Chen, X., Yang, H., and Wang, Y. (2017). Parametric study of passive design strategies for high-rise residential buildings in hot and humid climates: miscellaneous impact factors. *Renewable and Sustainable Energy Reviews*, vol. 69(March), pp. 442–460. Available: https://doi.org/10.1016/j.rser.2016.11.055

Chen, X., & Yang, H. (2017). A multi-stage optimization of passively designed high-rise residential buildings in multiple building operation scenarios. *Applied Energy*, vol. 206, pp. 541–557. Available: https://doi.org/10.1016/j.apenergy.2017.08.204

Pang, Z., O'Neill, Z., Li, Y., & Niu, F. (2020). The role of sensitivity analysis in the building performance analysis: A critical review. *Energy and Buildings*, vol. 209, 109659. Available: https://doi.org/10.1016/j.enbuild.2019.109659

Cao, X., Wang K., Xia L., Yu W., Li B., Yao J., and Yao R. (2022). A three-stage decision-making process for cost-effective passive solutions in office buildings in the hot summer and cold winter zone in China. *Energy and Buildings*, vol. 268(August), 112173. Available: https://doi.org/10.1016/j.enbuild.2022.112173

Moazami, A., Nik, V. M., Carlucci, S., & Geving, S. (2019). Impacts of future weather data typology on building energy performance – Investigating long-term patterns of climate change and extreme weather conditions. *Applied Energy*, vol. 238, pp. 696–720. Available: https://doi.org/10.1016/j.apenergy.2019.01.085

Yanni, C. (2019). *Living on Campus: An Architectural History of the American Dormitory*, University of Minnesota Press: Minneapolis.

Wilson, A. (2021). Passive survivability. *Climate Adaptation and Resilience Across Scales*, Routledge: New York, NY, USA, pp. 141-152.

Morillón-Gálvez, D., Saldaña-Flores, R., and Tejeda-Martínez, A. (2004). Human bioclimatic atlas for mexico. *Solar Energy*, vol. 76(6), pp. 781–792. Available: https://doi.org/10.1016/j.solener.2003.11.008

Manzano-Agugliaro, F., Montoya, F. G., Sabio-Ortega, A., and García-Cruz, A. (2015). Review of bioclimatic architecture strategies for achieving thermal comfort. *Renewable and Sustainable Energy Reviews*, vol. 49 (September), pp. 736–755. Available: https://doi.org/10.1016/j.rser.2015.04.095

Watson, D. (1993). *The Energy Design Handbook*, The American Institute of Architects Press: Washington D.C.

DeKay, M., Brown, G. (2014).Sun, Wind, and Light: Architectural Design Strategies, John Wiley & Sons.

Roshan, Gh. R., Farrokhzad, M., & Attia, S. (2017). Defining thermal comfort boundaries for heating and cooling demand estimation in Iran's urban settlements. *Building and Environment*, vol. 121, pp. 168–189. Available: https://doi.org/10.1016/j.buildenv.2017.05.023

Ferrara, M., Fabrizio, E., Virgone, J., and Filippi, M. (2014). A simulation-based optimization method for cost-optimal analysis of nearly zero energy buildings. *Energy and Buildings*, vol. 84 (December), pp. 442–57. Available: https://doi.org/10.1016/j.enbuild.2014.08.031

Asadi, E., Silva, M. G., Antunes, C. H., and Dias, L. (2012). Multi-objective optimization for building retrofit strategies: a model and an application. *Energy and Buildings*, vol. 44 (January), pp. 81–87. Available: https://doi.org/10.1016/j.enbuild.2011.10.016

Saltelli, A., Tarantola, S., Campolongo, F., and Ratto, M. (2004). *Sensitivity analysis in practice: a guide to assessing scientific models*. John Willy & Sons, Ltd, Chichester; Hoboken, NJ, pp. 94–120. Available: https://archive.org/details/sensitivityanaly00salt

Menberg, K., Heo, Y., & Choudhary, R. (2016). Sensitivity analysis methods for building energy models: Comparing computational costs and extractable information. *Energy and Buildings*, vol. 133, pp. 433–445. Available: https://doi.org/10.1016/j.enbuild.2016.10.005

Morris, M. D. (1991). Factorial Sampling Plans for Preliminary Computational Experiments. *Technometrics*, vol. 33(2), pp. 161–174. Available: https://doi.org/10.1080/00401706.1991.10484804

Liu, S., Kwok, Y. T., Lau, K. K.-L., Ouyang, W., & Ng, E. (2020). Effectiveness of passive design strategies in responding to future climate change for residential buildings in hot and humid Hong Kong. *Energy and Buildings*, vol. *228*, 110469. Available: https://doi.org/10.1016/j.enbuild.2020.110469

Heiselberg, P., Brohus, H., Hesselholt, A., Rasmussen, H., Seinre, E., and Thomas, S. (2009). Application of sensitivity analysis in design of sustainable buildings. *Renewable Energy*, vol. 34(9), pp. 2030–2036. Available: https://doi.org/10.1016/j.renene.2009.02.016

Ruano, M. V., Ribes, J., Seco, A., and Ferrer, J. (2012). An improved sampling strategy based on trajectory design for application of the Morris method to systems with many input factors. *Environmental Modelling & Software*, vol. 37(November), pp. 103–109. Available: https://doi.org/10.1016/j.envsoft.2012.03.008

Campolongo, F., Cariboni, J., and Saltelli, A. (2007). An effective screening design for sensitivity analysis of large models. *Environmental Modelling & Software*, vol. 22(10), pp. 1509–1518. Available: https://doi.org/10.1016/j.envsoft.2006.10.004

Wang, S., Yi, Y. K., & Liu, N. (2021). Multi-objective optimization (MOO) for high-rise residential buildings' layout centered on daylight, visual, and outdoor thermal metrics in China. *Building and Environment*, vol. 205, 108263. Available: https://doi.org/10.1016/j.buildenv.2021.108263

Huang, C., Zhang, G., Yao, J., Wang, X., Calautit, J. K., Zhao, C., An, N., & Peng, X. (2022). Accelerated environmental performance-driven urban design with generative adversarial network. *Building and Environment*, vol. 224, 109575. Available: https://doi.org/10.1016/j.buildenv.2022.109575